



Cite this: *Nanoscale Adv.*, 2023, **5**, 3606

## Synthesis and application of polypyrrole nanofibers: a review

Yang Liu  <sup>\*a</sup> and Feng Wu <sup>\*bcd</sup>

State-of-the-art polypyrrole nanofiber-based nanoarchitectonics can be generally fabricated by electrospinning, interfacial polymerization and reactive template methods. Even though analogous nanofiber morphologies and nanofibrous network architectures can be obtained by these methods, the structural details and structural complexities may alter significantly as different synthesis methods are applied. For the electrospinning technique, on one hand, nanofibers can be directly obtained by spinning polypyrrole-containing dope solutions; on the other, the electrospun nanofiber mats can be used as templates to direct the nanofiber formation; a two-step fabrication process, including the electrospinning of polymer nanofiber mats and deposition of polypyrrole on the polymer nanofibers' surface, is generally employed. By tuning the electrospinning parameters, the composition, diameter, morphology, and alignment of the as-obtained electrospun nanofiber mat can be effectively controlled, which may allow the fabrication of polypyrrole nanofibers with sophisticated nanostructures and nanoarchitectures. Interfacial polymerization is capable of generating polypyrrole nanofibers without templates. It is speculated that the protonation and re-orientation of polypyrrole at the oil–water interface may decoil the polymer chains and transform them into more extended conformations, while the charged polymer chains more easily diffuse into the water phase and form a stable dispersion. Different from electrospinning, the reactive templates may drive the formation of polypyrrole nanofibers through either redox or protonation mechanisms.

Received 4th March 2023  
Accepted 7th June 2023

DOI: 10.1039/d3na00138e  
[rsc.li/nanoscale-advances](http://rsc.li/nanoscale-advances)

<sup>a</sup>Department of Biomedical Engineering, Sun Yat-sen University, Shenzhen, China 518107

<sup>b</sup>Yunnan Provincial Key Laboratory of Energy Saving in Phosphorus Chemical Engineering and New Phosphorus Materials, China

<sup>c</sup>Engineering Research Center of Biodegradable Plastics, Educational Commission of Yunnan Province, China

<sup>d</sup>Faculty of Chemical Engineering, Kunming University of Science and Technology, Kunming, Yunnan, China 650500. E-mail: liuyang56@mail.sysu.edu.cn; fengwu@kust.edu.cn



Dr Yang Liu obtained a bachelor's degree in textile chemistry from Donghua University in 2009 and a master's degree in polymer and fiber engineering from Auburn University (supervisor: Prof. Dr Xinyu Zhang). He completed his PhD training in textile chemistry in The Hong Kong Polytechnic University (supervisor: Prof. Dr John H. Xin) in 2017 and became a research associate professor in

Sun Yat-sen University after graduation. His main research interest includes self-assembly of functional conducting polymer nanostructures, fast synthesis of conducting polymer nanocomposites for electrocatalysts using microwaves, and conductive interpenetrating network hydrogel for implantable electrodes and tissue engineering.



Dr Feng Wu has been an associate professor in the Department of Chemical Engineering, Kunming University of Science and Technology, China since 2021. His research interest includes sustainable polymer synthesis and modification, investigation of processing–structure–property relationships in polymer science, and developing functional polymers for agricultural applications. Dr

Feng Wu has authored/co-authored 47 peer-reviewed research articles, been awarded/has applied for more than 10 patents, and made several presentations in the international conferences. He serves in the editorial board of "Composites Part C: Open Access" and "Sustainable Polymer & Energy".



Nanofibers with different curvatures, compositions, and architectures can be obtained by using different types of reactive template in a simple, fast, environment-friendly and one-step manner. A wide range of applications have been demonstrated by the polypyrrole nanofiber-based nanoarchitectonics, including cell culture, tissue engineering, neural stimulation, energy storage, and organic electronics.

## 1. Introduction

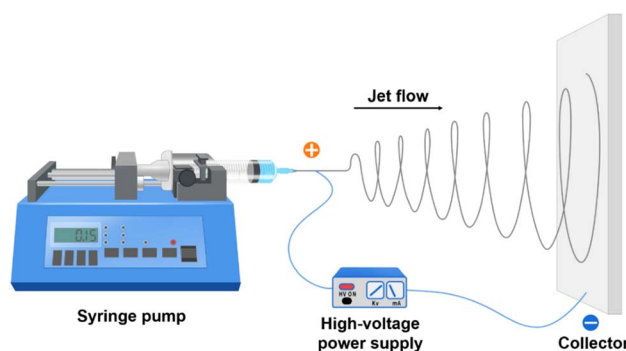
Nanofibers of the intrinsically conductive polymer polypyrrole have demonstrated their applied functions spanning a wide range of engineering fields, *e.g.*, supercapacitors, sensors, electromagnetic shielding, tissue engineering, neural stimulation, and neural regeneration.<sup>1–6</sup> The superior functional performance of polypyrrole nanofibers can be ascribed to their high specific surface area, interpenetrating network structure, high electrochemical activity, tunable band gap, and biocompatibility. Different techniques have been applied to synthesize polypyrrole nanofibers, including electrospinning, interfacial polymerization, soft templating, and seeding.<sup>7–10</sup> In order to obtain polypyrrole nanofiber products with high specific surface area, appropriate electronic structure, and good mechanical properties, the length, diameter, flexibility, morphology, and conductivity of the nanofibers should be controlled carefully and effectively. Moreover, the as-obtained polypyrrole nanofibers can be assembled into 1D, 2D, and 3D microstructures, *e.g.*, microfibers, sheets and membranes, in a continuous manner, making them attractive for the large-scale production of nanoarchitectonics with hierarchical nano-micro-geometries.<sup>11</sup> Different from conventional nanotechnology, nanoarchitectonics feature the harmonization of multiple, multiscale, and complex processes and interactions in the molecular, nano, and micro-scale to create life-like morphologies and functions.<sup>12</sup> Recently, new polypyrrole nanoarchitectonics with different micro–nano-structures and interfacial compositions, such as polypyrrole/metal halide/DNA hybrids,<sup>13</sup> polypyrrole hollow foam loaded with high-density MOF nanowires,<sup>14</sup> and polypyrrole:polystyrene sulfonate/cellulose nano-paper,<sup>15</sup> have emerged, showing promising applications in biosensors and wearable supercapacitors. Generally speaking, the fabrication of polypyrrole nanofibers may involve the synergy of free-radical polymerization, hydrophobic interaction, formation of a nano–micro-interface by nanofiber self-assembly *etc.* Harmonization of the synthesis processes may create nanofiber architectures with fractal geometries, where self-similar fibrous structures can be observed both microscopically and macroscopically. However, the existing techniques are diverse in the mechanisms, materials, and methods to produce polypyrrole nanofibers, so a review of and comparison between the existing techniques are necessary for understanding their characteristics, pros and cons, and differences, in order to rationally design the structural and nano-architectural features of polypyrrole nanofibers for engineering applications.

## 2. Electrospinning

Electrospinning has been widely used to fabricate electrospun nanofiber mats of different polymeric materials, providing the polymer can be properly dissolved in a solvent to make a dope

solution.<sup>16</sup> During the electrospinning process, the dope solution is loaded into a reservoir equipped with a blunt-needle-type outlet. To start electrospinning, the dope solution is ejected through the outlet at a constant flow rate by applying pressure and a voltage of up to 50 kV is applied to the needle. As a result of the applied voltage, charges will accumulate on the surface of the liquid meniscus at the needle tip, ejecting a continuous liquid jet from the meniscus, forming a hydrodynamic structure called a Taylor cone.<sup>17</sup> The liquid jet will move towards the collector, which is grounded or negatively charged, and placed several centimeters away from the needle tip. During the movement, the liquid jet will split, stretch, and solidify, forming nanofibers that randomly deposit on the surface of the collector; a schematic illustration of the electrospinning process of nanofibers is shown in Scheme 1. To obtain nanofiber mats with desired morphologies, structures, pore size distributions, sizes, and thicknesses, the electrospinning parameters, including the viscosity, surface tension, applied voltage, flow rate, needle size, needle/collector distance, collector dimensions, temperature and relative humidity, should be controlled carefully. Electrospinning might be the most versatile technique for fabricating nanofibers with different compositions, morphologies, structures and functions. It has been used extensively to fabricate different types of polypyrrole nanofibers, and the polypyrrole nanofiber membranes obtained from electrospinning have been used in a wide range of applications, *e.g.*, cell culture, tissue engineering, cancer therapy, biosensors, and supercapacitors.<sup>18–22</sup>

However, pure polypyrrole nanofibers cannot be obtained directly when the electrospinning techniques are used. Additional coating steps to form a polypyrrole layer on the surface of the electrospun nanofibers are required when polymer solutions not containing polypyrrole are used as the dope solution for electrospinning. On the other hand, pure polypyrrole is difficult to be electrospun into nanofibers due to its low solubility and dispersability. Additives such as co-solvents,



Scheme 1 Illustration of the electrospinning process.

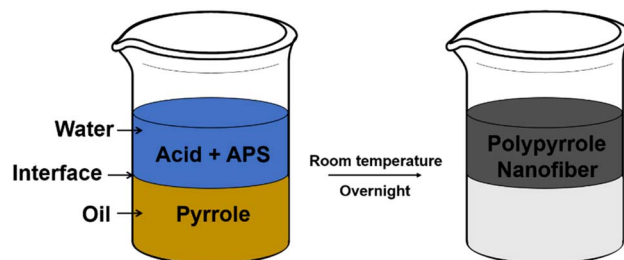


surfactants, and polymer carriers are needed to prepare polypyrrole solutions that are suitable for electrospinning,<sup>23,24</sup> which may significantly alter the conductivity of the nanofibers. Many attempts have been made to circumvent the obstacle of polypyrrole solubility, for example, polypyrrole with improved solubility in organic solvents was synthesized by the addition of functional dopants, *i.e.*, [di(2-ethylhexyl)sulfosuccinic acid sodium salt], butylnaphthalene sulfonic acid sodium salt, and dodecylbenzene sulfonic acid sodium salt;<sup>25</sup> upon further functionalization with chlorosulfonic acid, the water solubility of the as-obtained polypyrrole can reach 3 wt%, due to which it can be utilized for the electrospinning process in the aqueous phase.<sup>26</sup> E. Tavakkol *et al.* reported the fabrication of electrospun polypyrrole nanofibers by spinning the mixture solution of pyrrole and poly(vinylpyrrolidone) (PVP) into an ethanolic solution of  $\text{FeCl}_3$ .<sup>27</sup> The addition of PVP into the spinning dope solution can remarkably increase its viscosity and enhance the spinnability, but a second polymerization step was required to convert the pyrrole/PVP nanofibers into polypyrrole/PVP nanofibers, which may significantly affect the diameters and conductivities of the nanofibers.

Even though electrospinning has been proven to be one of the most versatile techniques to generate polymer nanofiber membranes and composites, it may require precise control over a wide range of processing parameters to achieve continuous and bead-free production of nanofibers, and the tuning of the parameters, *e.g.*, applied voltage, viscosity, temperature and relative humidity, is tedious and empirical, which may lower the efficiency of the fabrication process. High applied voltages and organic solvents are used during the electrospinning process, which may make it energy-consuming and environment-polluting. Nanofibers obtained from electrospinning may have a relatively wide range of size distribution and it is hard to obtain monodisperse nanofibers.

### 3. Interfacial polymerization

Polypyrrole nanofibers can be directly obtained from the free-radical polymerization of pyrrole through interfacial polycondensation. In a typical process, pyrrole is dissolved in an organic phase, *e.g.*, xylene, carbon disulfide, carbon tetrachloride, chloroform, methylene chloride, or toluene, while a strong acid (*e.g.*, 1 M hydrochloric acid) and a persulfate-type initiator [*e.g.*, ammonium persulfate (APS)] are mixed homogeneously to form the aqueous phase. To initiate the interfacial polymerization process, the water phase is carefully transferred to the top of the organic phase in a container, or *vice versa*, depending on the difference in density between these two phases. Due to the immiscibility of the two phases, an oil–water interface would form and the formation of the polypyrrole nanofibers may occur by the diffusion of the pyrrole monomer from the organic solvent to the aqueous phase *via* the oil–water interface. The interfacial polymerization can proceed at room temperature and the reaction occurs overnight to obtain polypyrrole nanofibers with sufficient degrees of polymerization and well-developed nanofibrous morphologies. Moreover, the as-obtained nanofibers can be assembled into a nanofibrous

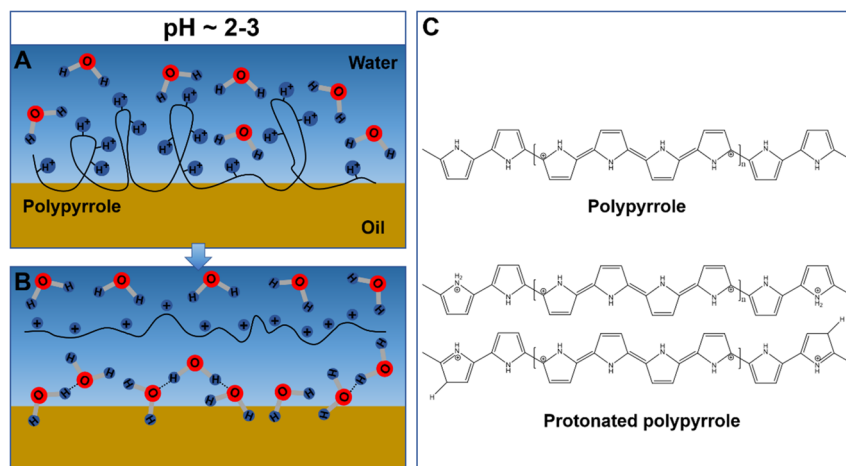


Scheme 2 Illustration of the synthesis of polypyrrole nanofibers by interfacial polymerization.

membrane by using a simple suction-filtration process. A schematic illustration of the interfacial polymerization process is shown in Scheme 2.

Compared to the fabrication of polypyrrole nanofibers by using electrospinning, where the electrospun nanofibers can be used as the hard template, no specific templates are required for the fabrication of polypyrrole nanofibers *via* interfacial polymerization. It is speculated that the formation of the nanofibrous morphology is closely related to the adsorption, orientation and desorption of the polypyrrole molecules at the oil–water interface and is highly pH-dependent. The pH-dependent adsorption/desorption process of polyelectrolytes has been investigated by D. K. Beaman *et al.*, who showed the change in pH can significantly alter the conformation of the polyelectrolytes, as a result of the increased charge density in the polymer backbone; the charge accumulation in the backbones would induce the intra/inter-molecular repulsion of the polymer, driving the swell and de-coil of the polymer chains, forming more extended and linear conformations; the charges in the polymer backbone can promote the ionization of the neighboring groups and reduce the free energy of desorption, and the entire polymer chain may move to the bulk water when a substantial portion of it is solvated and the free energy of desorption is sufficiently low.<sup>28</sup> The formation of the polypyrrole nanofibers through interfacial polymerization can also be explained by the pH-dependent adsorption/desorption of the polypyrrole chains at the oil–water interface. Briefly speaking, when the water phase containing acids and initiators is spread on top of the oil phase containing pyrrole, the pyrrole monomers adsorbed at the oil–water interface would be oxidized by the persulfate ions, forming pyrrole radicals and polymerizing through free radical polymerization. Simultaneously, the as-obtained polypyrrole chains would be protonated by the protons adsorbed at the oil–water interface. Q. Pei *et al.* reported that polypyrrole can be partially protonated in an aqueous solution with pH around 2–3,<sup>29</sup> which is consistent with the pH value of the aqueous phase used for the interfacial polymerization. As a result of the electrostatic repulsion, the protonated polypyrrole chains would adopt a more linear and extended conformation instead of the random coil conformation, which may promote the formation of nanofibers; the charges distributed along the protonated polypyrrole chains can reduce the free energy of desorption and promote the solvation of the as-formed nanofibers in the bulk water phase. Short and





**Scheme 3** pH-dependent adsorption and desorption of polypyrrole at the oil–water interface. Polypyrrole is firstly protonated by the protons ( $H^+$ ) at pH  $\sim 2$ –3 (A), and subsequently adopts an extended conformation as a result of the electrostatic interaction, and desorbs from the oil–water interface due to a reduction in free energy (B). (C) The chemical structures of the pristine polypyrrole and protonated polypyrrole.

curved nanofibers with small diameters (10–80 nm) can be formed by using interfacial polymerization.<sup>30–32</sup> However, by harmonizing the electrochemical and interfacial polymerization techniques, polypyrrole nanofiber arrays with controllable nanofiber lengths can be obtained.<sup>33</sup> A schematic illustration of the pH-dependent adsorption/desorption process of polypyrrole at the oil–water interface is shown in Scheme 3.

The addition of surface-active reagents, *e.g.*, surfactants, during the interfacial polymerization may significantly alter the morphology of the polypyrrole nanofibers. Recently, Z. Hou *et al.* investigated the effect of the hydrophilic–lipophilic balance (HLB) value on the morphology of polypyrrole synthesized by interfacial polymerization.<sup>34</sup> The HLB value was tuned by mixing different proportions of Span80 and OP10 to make a mixture surfactant. The mixture surfactant and  $FeCl_3$  were dissolved in water to make the aqueous phase, while pyrrole was

dissolved in chloroform to make the oil phase. As the HLB value of the mixture surfactant increased from 4.3 to 14.5, the morphology of the as-obtained polypyrrole changed from ruptured vesicle-like (Fig. 1A and B) to network-like (Fig. 1C and D) and to coral-like (Fig. 1E and F), respectively. The formation of the network-like structure at HLB = 10.4 indicated that the mixture surfactant in this case was more effective in de-coiling and stabilizing the polypyrrole chains at the interface. However, the formation of a primitive network-like structure instead of a well-defined nanofibrous interpenetrating network in the absence of a strong acid indicates that the protonation and extension of the polypyrrole chains under acidic conditions is vital in promoting the nanofiber formation.

The morphology of polypyrrole synthesized by interfacial polymerization is very sensitive to the synthesis conditions. H. Albaris *et al.* reported the use of interfacial polymerization to

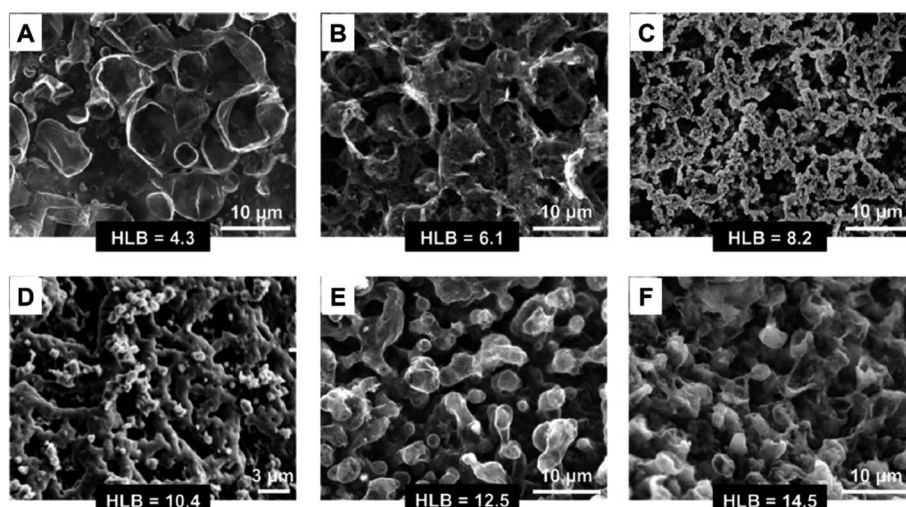


**Fig. 1** Changes in the morphology of polypyrrole synthesized by interfacial polymerization with the addition of mixture surfactants with different HLB values. The morphologies of the as-synthesized polypyrrole alter from ruptured vesicle-like (A and B) to network-like (C and D), and eventually to coral-like (E and F) as the HLB value of the surfactant increased. Reproduced from ref. 34, with permission from Elsevier, 2018.



synthesize polypyrrole and polyaniline.<sup>35</sup> During the synthesis, pyrrole or aniline was dissolved in carbon tetrachloride along with HCl and cetyltrimethylammonium bromide (CTAB) to make the oil phase, while APS was dissolved in water to make the aqueous phase. However, only particulate aggregates were obtained after the polymerization, indicating the addition of HCl and CTAB in the oil phase was unfavorable for the nanofiber formation. This phenomenon can be mainly attributed to the polymerization of pyrrole catalyzed by diluted HCl,<sup>36</sup> which may generate polydisperse polypyrrole nanospheres as the nucleation centers to induce the growth of polypyrrole particles. Polypyrrole nanofibers can also be obtained by conducting the interfacial polymerization at the interfaces formed between the oil droplets and bulk water. J. Hazarika *et al.* reported the synthesis of polypyrrole nanofibers by dispersing the xylene droplets containing pyrrole into the water phase containing *p*-toluenesulfonic acid (*p*-TSA) and APS under constant stirring in ambient conditions.<sup>37</sup> Compared to the nanofibers synthesized by using a static oil–water interface, the dispersed oil–water interface created by the constant stirring may result in a lower monomer concentration, a higher proton concentration, and a higher initiator concentration at the local oil–water interface between the oil droplets and the bulk water phase, where an increased polymerization rate can be observed, and a faster mass transport from the oil–water interface to the bulk water can also be expected, and eventually the formation of short nanofibers with small diameters was observed.

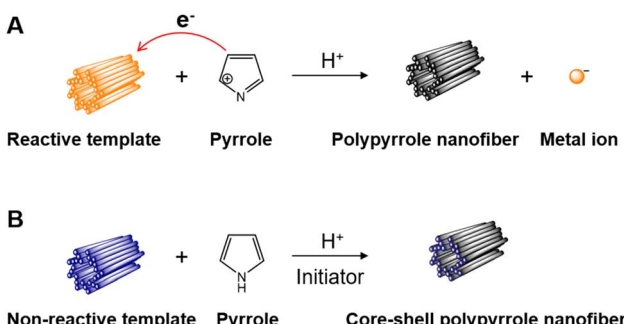
#### 4. Solution-based template methods

Polypyrrole nanofibers can be readily synthesized in aqueous solutions by using templates with 1D nanofibrous morphologies. The solution-based template methods have been proven to be simple, fast, and high-efficiency routes to fabricate polypyrrole nanofibers with versatile compositions, morphologies, and practical functions.<sup>38</sup> Based on the reactivity of the 1D nanofibrous templates with respect to the polymerization reaction of pyrrole, the templates can be categorized as reactive or non-reactive. During the polymerization process, the reactive templates can not only act as the replica molds to direct the formation of nanofibers, but can also serve as the initiators to trigger the polymerization of pyrrole. On the other hand, the

non-reactive templates can only serve as the replica molds for forming the nanofibers. A schematic illustration of the solution-based template method is shown in Scheme 4.

To date, ionic complexes and metal oxides have been mainly used as the reactive templates, and are capable of producing polypyrrole nanofibers that perfectly reflect their primitive morphologies. In 2005, A. Wu *et al.* reported the synthesis of polypyrrole nanofibers by using an ionic complex composed of CTAB and APS as a reactive template.<sup>39</sup> The synthesis was conducted in an aqueous solution containing 1 M HCl. A dense polypyrrole–nanofiber network composed of long and curved nanofibers can be obtained by using this method. The diameters of the nanofibers were in the range between 20 and 40 nm, and the nanofibers were randomly oriented, showing large curvatures (Fig. 2A). Formation of the highly curved polypyrrole nanofibers can be possibly attributed to the preferential 2D stacking of the CTAB–APS ionic complexes in the aqueous solution with a low pH,<sup>40</sup> which may form loosely packed lamellar micelles as the templates for nanofiber growth (Fig. 2B and C). However, to maintain the structure of the lamellar micelles, excess APS (molar ratio of CTAB : APS = 1 : 3) is required. Recently, K. Shu *et al.* developed a new “tandem” strategy to fabricate flexible thin-film composites of exfoliated graphene and polypyrrole nanofibers.<sup>41</sup> “Tandem” means the CTAB used to fabricate the exfoliated graphene is also used for the synthesis of polypyrrole nanofibers without removal. To obtain the composite of exfoliated graphene and polypyrrole nanofibers, pyrrole and concentrated HCl were added into the dispersion containing exfoliated graphene and CTAB, and subsequently APS was added to initiate the polymerization process. The polymerization was proceeded in an icy bath under magnetic stirring for 6 h, and subsequently flexible thin-film composites of exfoliated graphene and polypyrrole nanofibers can be obtained by simple suction filtration and washing processes. The as-obtained thin-film composite showed a thickness of around 10  $\mu\text{m}$ , which was composed of stacking layers of polypyrrole nanofibers intercalated with graphene sheets. Compared to the thin film composed solely of exfoliated graphene or polypyrrole nanofibers, the composite film showed enhanced mechanical properties, specific capacitance, and rate performance, which were important for supercapacitors.

On the other hand, nanostructured metal oxides that are able to initiate the free radical polymerization of pyrrole can be used to fabricate nanofibrous polypyrrole with different morphologies, compositions, and architectures. It has been recently reported by D. P. Dubal *et al.* that polypyrrole nanotubes, nanofibers, and urchins can be obtained by using manganese dioxide ( $\text{MnO}_2$ ) nanorods, nanofibers, and urchins as the reactive templates.<sup>42</sup> The synthesis process for the nanostructured polypyrrole was simple and straightforward: the nanostructured  $\text{MnO}_2$  was firstly dispersed in an aqueous solution of 1 M HCl, where pyrrole and the oxidant ( $\text{K}_2\text{Cr}_2\text{O}_7$ ) were subsequently added and the reactants were properly mixed. The polymerization was conducted at room temperature and nanostructured polypyrrole with the same morphologies as the  $\text{MnO}_2$  templates can be readily obtained (Fig. 3A and B). The  $\text{MnO}_2$  templates were simultaneously removed as the



Scheme 4 Illustration for the synthesis process of polypyrrole nanofibers using (A) a reactive template and (B) non-reactive template.



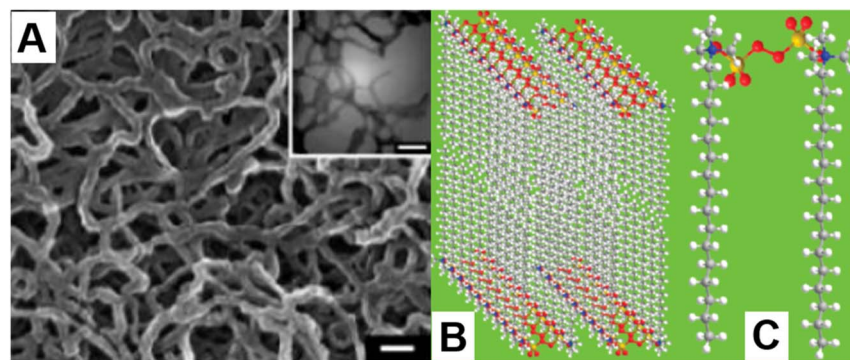
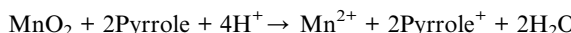


Fig. 2 Synthesis of polypyrrole nanofibers using the CTAB-APS ionic complex. (A) The morphology of the as-synthesized nanofibers. Reproduced from ref. 39, with permission from The American Chemical Society, 2005. (B) The 3D lamellar structure of the CTAB-APS complexes and (C) the 3D structure of a single CTAB-APS complex. Reproduced from ref. 40, with permission from The American Chemical Society, 2010.

polymerization process was completed, which can be attributed to the displacement reaction between  $\text{MnO}_2$  and pyrrole. As  $\text{MnO}_2$  has a higher oxidation potential ( $E = +1.224$  V)<sup>43</sup> than pyrrole ( $E = +0.7$  V),<sup>44</sup> it can be readily reduced by pyrrole, forming soluble  $\text{Mn}^{2+}$  cations and pyrrole radicals, which can be written as:



Excellent specific capacitance, cycling stability and rate performance were observed for the nanostructured polypyrrole synthesized using  $\text{MnO}_2$  as the reactive template due to the increased electrochemically active surface area, fast ion/electron transport, and enhanced interfacial redox reactions. For the nanostructured polypyrrole with different

morphologies, the nanofibers showed the best electrochemical properties for energy storage applications, possibly due to their ability to assemble into interconnected network architectures. Other than nanofibers solely composed of polypyrrole, core-shell nanofibers composed of a metal oxide core and a polypyrrole shell can also be obtained by using the reactive template. J. Wang *et al.* reported the fabrication of  $\text{V}_2\text{O}_5@\text{polypyrrole}$  core-shell nanowires by using  $\text{V}_2\text{O}_5$  nanowires as the reactive template.<sup>45</sup> The  $\text{V}_2\text{O}_5$  nanowires were firstly synthesized by a hydrothermal method and then dispersed in an aqueous solution of sodium dodecylbenzenesulfonate (NaDBS). The pH of the dispersion was adjusted to 1 using diluted  $\text{H}_2\text{SO}_4$  and the temperature was maintained at 0–5 °C by using an icy bath. Subsequently the polymerization process was started by adding pyrrole, which was oxidized by the  $\text{V}_2\text{O}_5$

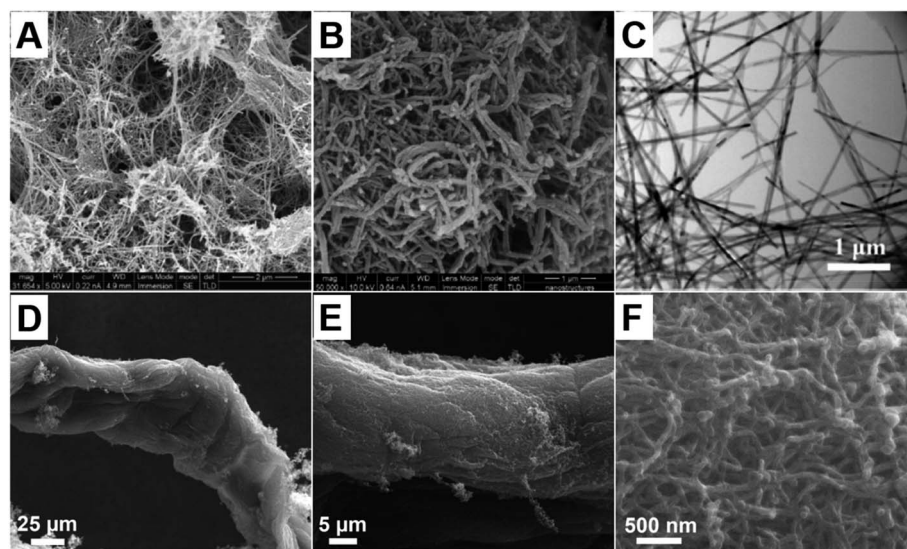


Fig. 3 Polypyrrole nanofibers synthesized by using nanostructured metal oxides as the reactive template. The morphologies of the  $\text{MnO}_2$  nanowire templates and the as-synthesized polypyrrole nanofibers are shown in (A) and (B), respectively. Reproduced from ref. 42, with permission from Elsevier, 2016. (C) TEM image showing the core–shell structure of the  $\text{V}_2\text{O}_5@\text{polypyrrole}$  nanowires. Reproduced from ref. 45, with permission from The American Chemical Society, 2018. (D) SEM image showing the morphology of the bulk polypyrrole fiber; microscale creases and folds can be observed on the fiber surface due to the applied stress during fiber formation. (E) The magnified morphology of the folding area, and (F) the morphology of the polypyrrole nanofibers that constitute the bulk fiber. Reproduced from ref. 46, with permission from The American Chemical Society, 2022.

nanowire templates and formed a polypyrrole layer on the surface of the nanowires. The TEM image of the  $\text{V}_2\text{O}_5$ @polypyrrole core–shell nanowires is shown in Fig. 3C, where the crystalline  $\text{V}_2\text{O}_5$  cores and the amorphous polypyrrole shells can be clearly distinguished. To ensure the formation of  $\text{V}_2\text{O}_5$ @polypyrrole core–shell nanowires and avoid the excess displacement of the  $\text{V}_2\text{O}_5$  cores by pyrrole, the molar ratio between  $\text{V}_2\text{O}_5$  and pyrrole was set at around 1:0.66. Compared to the samples consisting solely of  $\text{V}_2\text{O}_5$  nanowires or polypyrrole, the  $\text{V}_2\text{O}_5$ @polypyrrole core–shell nanowires showed remarkable improvements in specific capacitance, rate performance and cycling stability. Nanofiber dispersions and nanofibrous membranes composed of randomly oriented polypyrrole nanofibers can be obtained by the reactive template methods in general, while new nanoarchitectures are rarely reported. By adding low-molecular-weight polyethylene glycol (PEG) into the reactive template of  $\text{V}_2\text{O}_5$  nanofiber sol, bulk polypyrrole fibers composed of polypyrrole nanofibers assembled along the fiber long axis can be synthesized in a one-step manner.<sup>46</sup> This new nanoarchitecture of polypyrrole typically showed diameters in the range of 10–50  $\mu\text{m}$ , while their lengths can reach several centimeters. The surface of the bulk polypyrrole fibers is not smooth, and is roughened by intensive creases and folds that can span over several tens of microns (Fig. 3D). The SEM image with higher magnification shows the detailed morphology of the creases and folds, revealing a hierarchical micro/nano-structure composed of stacking layers of polypyrrole nanofibers (Fig. 3E). Moreover, the micro-creases and folds formed by the mismatch between the layers are observed to be partially aligned with the long axis of the fiber, which can be attributed to the shear stress applied on the  $\text{V}_2\text{O}_5$  nanofiber sol during the synthesis process. The surface nanostructure of the bulk polypyrrole fiber is shown in Fig. 3F, as a dense layer of interwoven polypyrrole nanofibers with an average diameter of 63 nm and a standard deviation of  $\pm 7$  nm can be observed. Compared to the polypyrrole nanofibers synthesized solely by  $\text{V}_2\text{O}_5$  nanofiber sol and polypyrrole granules synthesized without adding the  $\text{V}_2\text{O}_5$  sol, the bulk polypyrrole fibers showed enhanced electronic properties, *i.e.*, a larger band gap, a higher bipolaron density, and a higher degree of charge carrier delocalization, which can be ascribed to the strong hydrogen bonding and charge transfer interaction between the PEG molecules and polypyrrole.

Different from the reactive templates that drive the nanofiber formation through a redox mechanism, the nanofibrous templates that are able to protonate pyrrole monomers can also induce the formation of polypyrrole nanofibers. Pyrrole radicals can form by the protonation process, which can initiate the polymerization of pyrrole through a trimerization mechanism (Fig. 4). Polypyrrole nanofibers with unique helicity can be synthesized by using chiral amino acids as the template. For example, A. Xie *et al.* reported the use of left-handed and right-handed *N*-myristoyl-glutamic acids (L/R-MGA) to synthesize single-handed helical polypyrrole nanotubes with diameters of around 80 nm in an ethanol/water solution.<sup>47</sup> Polypyrrole nanotubes with either a left-handed helical structure or a right-handed helical structure can be obtained by using L-MGA or R-

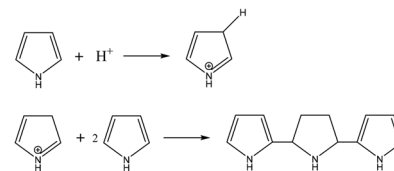


Fig. 4 Protonation and trimerization processes of pyrrole in acids.

MGA, respectively. Helical polypyrrole nanofibers with diameters of around 40 nm can also be obtained by replacing the MGA templates with a gel dispersion of *N*-myristoyl-L-diglutamic acid (L-MDGA). When being used as the electromagnetic interference (EMI) shielding materials, the helical nanostructured polypyrrole showed both high shielding efficiency and wide absorbing frequency range, while the highest absorption width of 7.04 GHz was obtained for the helical polypyrrole nanofibers in the frequency range between 10.6 and 17.64 GHz. By adding different acids into the polymerization solution of the helical polypyrrole nanotubes, M. Sun *et al.* were able to synthesize hollow polypyrrole nanofibers with tunable microstructures, which can be used for EMI shielding.<sup>48</sup>

On the other hand, electrospun nanofiber mats can also be used as either non-reactive or reactive templates to synthesize polypyrrole nanofibers. For example, R. Elashnikov *et al.* prepared polypyrrole nanofiber membranes for cell culture and stimulation by using an electrospun cellulose acetate butyrate (CAB) nanofiber mat as the substrate;<sup>49</sup> SEM images of the as-obtained CAB nanofiber mat are shown in Fig. 5A and B. Polypyrrole was then deposited onto the CAB nanofiber mat by chronopotentiometry. Both randomly oriented and uniaxially aligned polypyrrole nanofiber membranes can be obtained from the electrospinning process, by using either a single plate or parallel plates as the collector (Fig. 5C and D). The as-obtained polypyrrole nanofiber membranes can significantly promote the growth of the human neuroblastoma cells (SH-SY5Y) when electrical stimulation is applied, resulting in longer neurites with more branches. Compared to the randomly oriented nanofiber mat, the uniaxially aligned nanofiber mat can induce directional neurite growth, resulting in a higher average length for the as-grown neurites. Y. Zhou *et al.* reported the fabrication of a high-performance yarn-based strain sensor by using the polypyrrole nanofiber composites.<sup>50</sup> According to their method, a spandex yarn was pre-stretched and fixed in between two twisting rollers connected to a winding device. The graphene oxide (GO) doped polyacrylonitrile (PAN) nanofibers were then electrospun onto the spandex yarn and covered its surface. Subsequently the nanofiber coated yarn was twisted by the twisting rollers to entangle the nanofibers and the spandex yarn. After removing the stretching load, the nanofibers would contract to form a uniform wavy structure on the surface of the yarn, as shown in Fig. 5E and F. Polypyrrole was then deposited onto the surface of the PAN nanofiber-coated spandex yarn by a free radical polymerization process in the aqueous phase, forming a continuous conductive layer on the PAN nanofibers' surface, as shown in Fig. 5G and H. The as-obtained composite yarn was highly adaptable to the weaving process and showed



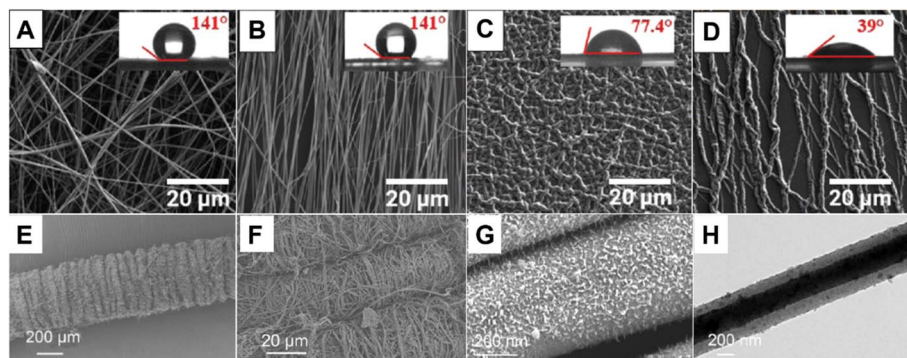


Fig. 5 SEM images of the electrospun CAB (A and B) and polypyrrole coated CAB nanofiber membranes (C and D) with either random (A and C) or uniaxially aligned (B and D) orientations. Insets show the water contact angles of the membranes, respectively. Reproduced from ref. 49, with permission from Royal Society of Chemistry, 2019. (E) SEM image of the polypyrrole/GO doped-PAN-nanofiber coated spandex yarn with a wavy surface texture. (F) The wavy surface texture is formed by the contraction of the nanofiber coating. (G and H) SEM and TEM images of the polypyrrole layer deposited on the GO doped PAN nanofiber surface. Reproduced from ref. 50, with permission from The American Chemical Society, 2022.

remarkable sensory properties when used as a strain sensor. Moreover, D. P. Bhattarai *et al.* reported the use of an electrospun polycaprolactone (PCL) nanofiber mat as a sacrificial template to fabricate hollow polypyrrole nanofibers.<sup>51</sup> Polypyrrole was deposited onto the surface of the PCL nanofiber mat by free radical polymerization to form a PCL/polypyrrole core-shell membrane. Subsequently the PCL core was dissolved in dichloromethane, leaving hollow polypyrrole nanofibers. The hollow polypyrrole nanofibers showed no toxicity against breast cancer cells (MCF7) under ambient conditions, while a strong photothermal toxicity against the MCF7 cells can be obtained by irradiating the nanofibers with an 808 nm near-infrared (NIR) light source. Compared to the polypyrrole nanoparticles, the hollow nanofibers showed much higher drug-loading capacity, which can be attributed to the hollow-fiber microstructure. Upon the incorporation of oxidants, electrospun nanofibers can also be used as reactive templates to prepare polypyrrole nanofibers. X. Lin *et al.* reported the fabrication of an all-nanofiber-based piezoresistive sensor by using polypyrrole coated electrospun nanofibers.<sup>52</sup> The sensor was composed of a polypyrrole/PVP/PAN nanofiber mat as the central layer, which was prepared by polymerizing pyrrole on the surface of the FeCl<sub>3</sub> containing electrospun PVP nanofibers. An electrospun thermoplastic polyurethane (TPU) nanofiber mat printed with interdigitated silver electrodes was used as the bottom layer, and an electrospun TPU nanofiber mat was used as the top layer. These layers were sandwiched to assemble the piezoresistive sensor, which showed excellent pressure sensing abilities against different body motions accompanied by good breathability and heat dissipation, making it a good candidate for electronic skins.

## 5. Structure–property correlations of the polypyrrole nanofibers

Polypyrrole nanofibers synthesized by using different methods have various structures and hence different properties.

Electrical conductivity is considered as one of the most important properties for conducting polymers, *e.g.*, polypyrrole, since the main applications of conducting polymers, such as in supercapacitors, organic solar cells, bioactive scaffolds, conductive fillers, and sensors, require high electrical conductivity to realize advanced functions and performance. The correlations between the electrical conductivities of the polypyrrole nanofibers and the corresponding synthesis methods in the literature are summarized in Table 1. From Table 1, it can be seen that the electrical conductivities of the nanofibers differ significantly based on the synthesis conditions, including the methods, morphologies, molar ratios, and dopants. By carefully investigating the detailed information and parameters in the literature, a few general rules can be deduced: (i) the electrical conductivity of the as-prepared nanofibers increases with the weight fraction of polypyrrole, especially for the electrospun nanofibers; (ii) the electrical conductivity of the polypyrrole nanofibers increases as the density of polypyrrole increases, *e.g.*, the conductivity of the solid polypyrrole nanofibers is generally higher than that of the hollow nanofibers or coatings; (iii) the conductivity of the as-prepared nanofibers depends on their composition, and the presence of other conductive components can enhance the electrical conductivity; (iv) organic dopants, such as benzenesulfonate anions, can induce higher electrical conductivity, which can be attributed to the electrostatic shielding effect originating from their large sizes; (v) protonation in the acidic solution may enhance the reactivity of pyrrole, resulting in the formation of polypyrrole with higher electrical conductivity. The unique nanofibrous morphology may provide anisotropic physical properties, larger surface area, and assemblability, which may significantly improve the efficiency of functionalization and nanoscale self-assembly. By taking advantage of the unique doping-induced properties of polypyrrole, *e.g.*, conductivity, structural change, and stimuli-responsiveness, important applications of polypyrrole nanofibers may be found across a wide range of research disciplines.



Table 1 Summary of the compositions, morphologies, and conductivities of the polypyrrole (PPy) nanofibers prepared by using different synthesis methods

Name	Synthesis method	PPy morphology	Molar ratio of Py to oxidant	Dopant	Conductivity	Testing method
PPy/chitosan/collagen nanofiber scaffold (15 wt% PPy) <sup>4</sup>	Electrospinning	Blended in the electro-spun nanofibers; $d_{\text{avg}} = 83.7 \text{ nm}$	0.95	Diethyl sulfosuccinate, $\text{SO}_4^{2-}$	$\sim 164 \times 10^{-3} \text{ S m}^{-1}$	4-Probe, sheet form
PPy nanofibers <sup>8</sup>	Interfacial polymerization	Nanofiber bundles and networks; diameter range: 75–180 nm	7.27 (0.3 for $\text{FeCl}_3$ )	$\text{HCl}, \text{FeCl}_3, p\text{-TSA, CSA, PSSA}$	<sup>b</sup> $25 \times 10^{-4}, 21 \times 10^{-4}, 6 \times 10^{-2}, 4 \times 10^{-2}, 20 \times 10^{-4} \text{ S cm}^{-1}$	4-Probe, pressed pellet
PPy nanoribbons and nanowires <sup>9</sup>	Reactive templating	Curved nanowire or nanoribbon networks; diameter: 20–65 nm	1	$\text{Br}^-, \text{SO}_4^{2-}$	$7.3 \times 10^{-3} \text{ S cm}^{-1}$	4-Probe, compressed pellet (10 MPa)
PPy/PVDF electrospun nanofibers <sup>20</sup>	Electrospinning	Blended in the electro-spun nanofibers; $d_{\text{avg}} = 325 \text{ nm}$	0.5	$\text{FeCl}_3$	$\sim 1.6 \times 10^{-4} \text{ S cm}^{-1}$	LCR meter, nanofiber membrane
$\text{MnO}_2@\text{PAA/PPy}$ core–shell composite fibers <sup>22</sup>	Reactive templating	Granular coating, 50 nm thick	—	$\text{FeCl}_3$	$1.19 \times 10^{-3} \text{ S m}^{-1}$	2-Probe, fiber mat
PPy/PEO nanofibers <sup>26</sup>	Electrospinning	Blended in the electro-spun nanofibers; diameter range: 200–300 nm	—	Organic acids	$4.9 \times 10^{-8}$ to $1.2 \times 10^{-5} \text{ S cm}^{-1}$ , depending on the PPy content	2-Probe, fiber mat
PPy/PVP nanofibers <sup>27</sup>	Electrospinning	Blended in the electro-spun nanofibers; $d_{\text{avg}} = 83 \text{ nm}$	—	$\text{AQSA, FeCl}_3$	$5.22 \times 10^{-1} \text{ S cm}^{-1}$	4-Probe, nano-fiber mat
PPy nanofibers <sup>37</sup>	Interfacial polymerization	Nanofiber bundles	1	$p\text{-TSA}$	$3.3 \times 10^{-1} \text{ S cm}^{-1}$	4-Probe, pressed pellet
PPy nanofibers <sup>37</sup>	Interfacial polymerization	Nanofiber bundles	1	$\text{HCl}$	$9.7 \times 10^{-2} \text{ S cm}^{-1}$	4-Probe, pressed pellet
Polypyrrole nanofibers <sup>39</sup>	Reactive templating	Nonwoven mat of nanofibers 2D nanoclips	4.3	$\text{SO}_4^{2-}, \text{Cl}^-, \text{Br}^-$	$\sim 100 \text{ S cm}^{-1}$	Compressed pellet
PPy nanoclips <sup>40</sup>	Reactive templating	4	$\text{SO}_4^{2-}, \text{Cl}^-, \text{Br}^-$	$2\text{--}5 \text{ S cm}^{-1}$	4-Probe, compressed pellet	
$\text{V}_2\text{O}_5@\text{PPy}$ core–shell nanowires <sup>45</sup>	Reactive templating	Nanocoating, 15 nm thick	0.65	$\text{DBS}^-, \text{SO}_4^{2-}$	—	—
PPy nanofiber assemblies <sup>46</sup>	Reactive templating	Uniaxially aligned bulk nanofiber assembly; $d_{\text{avg}} = 63 \text{ nm}$	3.27	$\text{SO}_4^{2-}, \text{Cl}^-$	$1.49 \text{ S m}^{-1}$	4-Probe, pressed pellet
PPy coated cellulose acetate butyrate nanofibers <sup>49</sup>	Non-reactive templating	Granular coating, 600 nm thick	—	$\text{H}_2\text{PO}_4^-$	$2.4 \times 10^{-5} \text{ S cm}^{-1}$	2-Probe, nano-fiber mat
Helical PPy nanofibers <sup>53</sup>	Non-reactive templating	Nanofibers with helical architectures; $d_{\text{avg}} = 113 \text{ nm}$	1	$\text{SO}_4^{2-}$	$1.83 \text{ S cm}^{-1}$	—
ANF-PVA-PPy hydrogel <sup>54</sup>	Non-reactive templating	Granular coating	—	$\text{FeCl}_3$	$\sim 80 \text{ S cm}^{-1}$	2-Probe, cuboid hydrogel

<sup>a</sup> Abbreviations:  $d_{\text{avg}}$  (average diameter),  $p\text{-TSA}$  (*p*-toluene sulfonic acid), CSA (camphor sulfonic acid), PSSA (polystyrene sulfonic acid), PVDF (polyvinylidene fluoride), PEO (polyethylene oxide), PVP (polyvinyl pyrrolidone), AQSA (anthraquinone-2-sulfonic acid sodium salt), DBS (dodecylbenzenesulfonate), ANF (aramid nanofibers), PVA (polyvinyl alcohol). <sup>b</sup> The conductivities of PPy nanofibers doped with HCl,  $\text{FeCl}_3$ ,  $p\text{-TSA}$ , CSA, and PSSA, respectively.

## 6. Emerging applications of polypyrrole nanofibers

### 6.1 Biomedical applications

Polypyrrole nanofibers have been researched for use in biomedical applications from medical diagnostics and drug delivery to tissue engineering and regeneration. Among them, drug delivery has long been researched, with the focus now shifting to PPy-based drug delivery systems with environmental stimuli-responsiveness including to pH and near-infrared (NIR).<sup>55</sup> Recently, synergistic therapy has also been developed for PPy-based drug delivery. For example, by encapsulating gold nanorods (GNRs) into polypyrrole (PPy) shells, photothermal and drug delivery performance for cancer therapy has been regulated.<sup>56</sup> Besides drug delivery, in recent years, a lot of research has been carried out on using PPy in medical diagnostics and tissue engineering. With the development of technologies such as toughening hydrogel, biodegradable polymers, biomimetics, and 3D printing, PPy nanofibers could find a wide range of applications in tissue engineering, as numerous studies have been carried out recently.<sup>57–60</sup>

### 6.2 Energy storage and conversion

The high surface area, good electrical conductivity, and excellent electrochemical performance make PPy suitable for enhancing energy storage and conversion efficiency, as it is widely used in energy storage devices such as supercapacitors and batteries. PPy holds great promise as a cathode material for fuel cells to replace noble metal catalysts, as it is capable of combining advanced functions including high oxygen-reduction activity, charge density and good performance durability, as reported by R. Bashyam *et al.*<sup>61</sup> The development of PPy-nanofiber synthesis technology will advance its application in fuel cells. Supercapacitors are another device in which PPy could play a great role. Flexible, stretchable, all-solid-state, fiber-shaped supercapacitors based on CNT-PPy fibers were fabricated, exhibiting high specific capacitance and excellent stretchable performance which could be used in wearable electronic devices.<sup>62</sup> A triboelectric nanogenerator (TENG) made from PPy has also been reported, and it showed a competitive performance comparable to that of commercial pulse sources.<sup>63</sup> It is expected that the PPy nanofibers will find great applications in energy storage and conversion systems, realizing enormous energy storage capabilities and promoting the commercialization of wearable devices, sustainable fuel cells and so on.<sup>64</sup>

### 6.3 Multifunctional actuators

With the increasing demand for integrated automatic machineries for repetitive industrial processes, it is of particular interest to develop advanced actuators for diverse applications ranging from robots and memory chips to micro-electromechanical systems (MEMS).<sup>65</sup> Compared to other materials, PPy actuators showed a high response strain rate, power density ( $\sim 39 \text{ W kg}^{-1}$ ), and stability when applying a potential up to 7 V within 1 s.<sup>66</sup> Electrical stimuli with low applied voltages

(electrochemical actuation) are the pros of the PPy based actuators, but challenges still exist, *e.g.*, how to simultaneously realize flexibility, durability, fast response and large stroke length. Hybridization of PPy with other carbon-based materials such as graphene and carbon nanotubes shows noticeable promise for constructing high-performance actuators.<sup>67</sup> Moreover, the incorporation of PPy into the wafer-scale nanoporous single-crystalline silicon membrane provided new perspectives for on-chip actuaries with outstanding voltage-strain coupling and small operation voltages.<sup>68</sup>

### 6.4 Sensors

Numerous studies have been conducted to develop PPy-based sensors, such as electrochemical, gas, and bio-sensors, since PPy is highly promising for commercial sensory applications as a result of its solution-processability, stimuli-responsiveness, and good environmental stability.<sup>69</sup> For biosensors, the analysis of selected DNA sequences and mutated genes associated with human disease is of significant importance. PPy may serve as a facile, high-performance and inexpensive functional material for fulfilling this goal. For example, a polypyrrole-based DNA chip has been designed and applied to the analysis of genomic DNA originating from cell lines and human colorectal samples, while practical features, such as low cost, high accuracy, and adaptability, can be realized.<sup>70</sup> Because of its high conductivity and electrochemical activity, PPy has been integrated with different substrates for collecting acute signals such as from genes,<sup>71</sup> ammonia gas, thermal heating, NIR light,<sup>72</sup> and volatile organic compounds.<sup>73</sup>

## 7. Conclusions

Polypyrrole nanofibers with different compositions, nano-architectures and combinations can be synthesized by using electrospinning, interfacial polymerization, and solution-based template methods. For the electrospinning method, the electrospun nanofiber mats can be utilized as the substrate for polypyrrole deposition and as the templates to direct nanofiber formation. A variety of polypyrrole nanofiber-based nano-architectures can be facilely fabricated by the electrospinning technique, including core-shell nanofibers, hollow nanofibers, and uniaxially aligned nanofibers. Moreover, advanced fiber/nanofiber-based composites and devices can be fabricated by coating polypyrrole on the surface of the composite nanofibers prepared by the electrospinning of a multi-component dope solution or co-electrospinning of different dope solutions. Enhanced electrical conductivity, charge storage capacity, photothermal properties and biocompatibility can be provided by the polypyrrole coating layer, while enhanced mechanical properties, processability, and wearability can be provided by the electrospun nanofiber substrates. Given the diversity in composition, nanoarchitecture and combination, the polypyrrole nanofiber-based nanoarchitectonics show promising performance in a wide range of applications, *e.g.*, cell culture, neural stimulation, photothermal therapy, electronic skins, and strain sensors.



Compared to the electrospinning technique, interfacial polymerization can generate polypyrrole nanofibers without the presence of a template. It is speculated that a pH-dependent adsorption/desorption process at the oil–water interface may drive the formation of the nanofibers. As the polymer chains of polypyrrole are protonated, de-coiled, and desorbed into bulk water at the oil–water interface, the as-obtained polypyrrole may take up more extended and linear conformations, forming a stable dispersion in water due to the electrostatic repulsion. Consequently, curved polypyrrole nanofibers with small diameters are generally obtained by interfacial polymerization. On the other hand, the conformation of the polymer chains can be effectively tuned in the presence of the oil–water interface, which may enhance the stacking order of the polymer chains, resulting in a higher crystallinity and conductivity.

Compared to the interfacial polymerization and electrospinning technique, the synthesis of polypyrrole nanofibers by using reactive templates does not require complicated spinning devices, post-spinning deposition, or tedious interfacial adsorption/desorption processes, and the synthesis process can be completed in a simple, fast, and environment-friendly manner. Different from the non-reactive templates, the reactive templates can initiate the polymerization of pyrrole through redox mechanisms, driving the formation of polypyrrole on their surface and forming polypyrrole that duplicates their nanofibrous morphologies. Polypyrrole nanofibers with versatile morphologies and nanoarchitectures can be obtained by using the reactive templates, including the highly curved nanofibers, long and straight nanofibers, nanotubes, core–shell nanofibers, nanofiber urchins, and hierarchical polypyrrole bulk fibers, which show a wide range of applications in supercapacitors, lithium-ion batteries, organic electronics, and EMI shielding.

## Conflicts of interest

The authors declare no conflicts of interest.

## Acknowledgements

The author gratefully acknowledges the financial support from the National Natural Science Foundation of China (81801851).

## References

- 1 K. Shi and I. Zhitomirsky, Polypyrrole nanofiber–carbon nanotube electrodes for supercapacitors with high mass loading obtained using an organic dye as a co-dispersant, *J. Mater. Chem. A*, 2013, **1**, 11614–11622.
- 2 J. Huang, J. Li, X. Xu, L. Hua and Z. Lu, In situ loading of polypyrrole onto aramid nanofiber and carbon nanotube aerogel fibers as physiology and motion sensors, *ACS Nano*, 2022, **16**, 8161–8171.
- 3 M. Parit, H. Du, X. Zhang, C. Prather, M. Adams and Z. Jiang, Polypyrrole and cellulose nanofiber based composite films with improved physical and electrical properties for electromagnetic shielding applications, *Carbohydr. Polym.*, 2020, **240**, 116304.
- 4 M. Zarei, A. Samimi, M. Khorram, M. M. Abdi and S. I. Golestaneh, Fabrication and characterization of conductive polypyrrole/chitosan/collagen electrospun nanofiber scaffold for tissue engineering, *Int. J. Biol. Macromol.*, 2021, **168**, 175–186.
- 5 J. Y. Lee, C. A. Bashur, A. S. Goldstein and C. E. Schmidt, Polypyrrole-coated electrospun PLGA nanofibers for neural tissue applications, *Biomaterials*, 2009, **30**, 4325–4335.
- 6 L. Yan, B. Zhao, X. Liu, X. Li, C. Zeng, H. Shi, X. Xu, T. Lin, L. Dai and Y. Liu, Aligned nanofibers from polypyrrole/graphene as electrodes for regeneration of optic nerve via electrical stimulation, *ACS Appl. Mater. Interfaces*, 2016, **8**, 6834–6840.
- 7 R. Guo, W. Guo, H. Pei, B. Wang, X. Guo, N. Liu and Z. Mo, Polypyrrole deposited electrospun PAN/PEI nanofiber membrane designed for high efficient adsorption of chromium ions (IV) in aqueous solution, *Colloids Surf. A Physicochem. Eng. Asp.*, 2021, **627**, 127183.
- 8 S. Goel, N. A. Mazumdar and A. Gupta, Synthesis and characterization of polypyrrole nanofibers with different dopants, *Polym. Adv. Technol.*, 2010, **21**, 205–210.
- 9 X. Zhang, J. Zhang, W. Song and Z. Liu, Controllable synthesis of conducting polypyrrole nanostructures, *J. Phys. Chem. B*, 2006, **110**, 1158–1165.
- 10 X. Zhang and S. K. Manohar, Bulk synthesis of polypyrrole nanofibers by a seeding approach, *J. Am. Chem. Soc.*, 2004, **126**, 12714–12715.
- 11 K. Ariga, Nanoarchitectonics: what's coming next after nanotechnology?, *Nanoscale Horiz.*, 2021, **6**, 364.
- 12 K. Ariga, Nanoarchitectonics: a navigator from materials to life, *Mater. Chem. Front.*, 2017, **1**, 208.
- 13 W. Ma, H. Du, M. Zhang, J. Mori, X. Ren, H. Wang and X. Zhang, One-step synthesis of tunable zinc-based nanohybrids as an ultrasensitive DNA signal amplification platform, *ACS Appl. Mater. Interfaces*, 2020, **12**, 2983–2990.
- 14 T. Yue, A. I. Douka, K. Qi, Y. Qiu, X. Guo and B. Xia, Flexible and hollow polypyrrole foam with high loading of metal-organic framework nanowires for wearable supercapacitors, *J. Mater. Chem. A*, 2021, **9**, 21799–21806.
- 15 Y. Liang, Z. Wei, H. Wang, R. Wang and X. Zhang, Flexible freestanding conductive nanopaper based on PPy:PSS nanocellulose composite for supercapacitors with high performance, *Sci. China Matter.*, 2023, **66**, 964–973.
- 16 A. Frenet and I. S. Chronakis, Polymer nanofibers assembled by electrospinning, *Curr. Opin. Colloid Interface Sci.*, 2003, **8**, 64–75.
- 17 D. H. Reneker and A. L. Yarin, Electrospinning jets and polymer nanofibers, *Polymer*, 2008, 2387–2425.
- 18 A. I. Yardimci, O. Baskan, S. Yilmaz, G. Mese, E. Ozcivici and Y. Selamet, Osteogenic differentiation of mesenchymal stem cells on random and aligned PAN/PPy nanofibrous scaffolds, *J. Biomater. Appl.*, 2019, **34**, 640–650.
- 19 W. Zhong, Q. Liu, Y. Wu, Y. Wang, X. Qing, M. Li, K. Liu, W. Wang and D. Wang, A nanofiber based artificial



electronic skin with high pressure sensitivity and 3D conformability, *Nanoscale*, 2016, **8**, 12105–12112.

20 P. Sengupta, A. Ghosh, N. Bose, S. Mukherjee, A. R. Chowdhury and P. Datta, A comparative assessment of poly(vinylidene fluoride)/conducting polymer electrospun nanofiber membranes for biomedical applications, *J. Appl. Polym. Sci.*, 2020, **137**, e49115.

21 J. Huang, J. Li, X. Xu, L. Hua and Z. Lu, In situ loading of polypyrrole onto aramid nanofiber and carbon nanotube aerogel fibers as physiology and motion sensors, *ACS Nano*, 2022, **16**, 8161–8171.

22 X. Lu, C. Shen, Z. Zhang, E. Barrios and L. Zhai, Core-shell composite fibers for high-performance flexible supercapacitor electrodes, *ACS Appl. Mater. Interfaces*, 2018, **10**, 4041–4049.

23 I. Masmur, S. Perangin-angin, H. Sembiring, A. H. Tarigan, J. Ginting, D. A. Barus and M. Ginting, Effect of different composition of polyethylene oxide-polypyrrole (PEO-PPY) nanofiber mats on antibacterial and biocompatibility properties, *ChemistrySelect*, 2022, **7**, e202201346.

24 Y. Cong, S. Liu and H. Chen, Fabrication of conductive polypyrrole nanofibers by electrospinning, *J. Nanomater.*, 2013, 148347.

25 K. S. Jang, H. Lee and B. Moon, Synthesis and characterization of water soluble polypyrrole doped with functional dopants, *Synth. Met.*, 2004, **143**, 289–294.

26 I. S. Chronakis, S. Grapenson and A. Jakob, Conductive polypyrrole nanofibers via electrospinning: electrical and morphological properties, *Polymer*, 2006, **47**, 1597–1603.

27 E. Tavakkol, H. Tavanai, A. Abdolmaleki and M. Morshed, Production of conductive electrospun polypyrrole/poly(vinyl pyrrolidone) nanofibers, *Synth. Met.*, 2017, **231**, 95–106.

28 D. K. Beaman, E. J. Robertson and G. L. Richmond, Ordered polyelectrolyte assembly at the oil-water interface, *Proc. Natl. Acad. Sci. U. S. A.*, 2012, **109**, 3226–3231.

29 Q. Pei and R. Qian, Protonation and deprotonation of polypyrrole chain in aqueous solutions, *Synth. Met.*, 1991, **45**, 35–48.

30 J. Huang and R. B. Kaner, A general chemical route to polyaniline nanofibers, *J. Am. Chem. Soc.*, 2004, **126**, 851–855.

31 C. Yin, G. Duan and W. Cai, Polyaniline nanofibers and their self-assembly into a film to be used as ammonia sensor, *RSC Adv.*, 2016, **6**, 103185–103191.

32 D. Xu, L. Fan, L. Gao, Y. Xiong, Y. Wang, Q. Ye, A. Yu, H. Dai, Y. Yin, J. Cai and L. Zhang, Micro-nanostructured polyaniline assembled in cellulose matrix via interfacial polymerization for applications in nerve regeneration, *ACS Appl. Mater. Interfaces*, 2016, **8**, 17090–17097.

33 M. Li, Z. Wei and L. Jiang, Polypyrrole nanofiber arrays synthesized by a biphasic electrochemical strategy, *J. Mater. Chem.*, 2008, **18**, 2276–2280.

34 Z. Hou, H. Lu, Q. Yang, Q. Zhao and J. Liu, Micromorphology-controlled synthesis of polypyrrole films by using binary surfactant of Span80/OP10 via interfacial polymerization and their enhanced electrochemical capacitance, *Electrochim. Acta*, 2018, **265**, 601–608.

35 H. Albaris and G. Karuppasamy, Inspection of room temperature hydrogen sensing property of nanostructured polypyrrole/polyaniline hetero-junctions synthesized by one-pot interfacial polymerization, *Mater. Chem. Phys.*, 2020, **250**, 123153.

36 S. J. Hawkins and N. M. Ratcliffe, A study of the effects of acid on the polymerisation of pyrrole, on the oxidative polymerisation of pyrrole and on polypyrrole, *J. Mater. Chem.*, 2000, **10**, 2057–2062.

37 J. Hazarika and A. Kumar, Scalable and low cost synthesis of highly conducting polypyrrole nanofibers using oil-water interfacial polymerization under constant stirring, *J. Phys. Chem. B*, 2017, **121**, 6926–6933.

38 S. Ghosh, *Conjugated Polymer Nanostructures for Energy Conversion and Storage Applications*, Wiley, Weinheim, Germany, 2021, ch. 2.

39 A. Wu, H. Kolla and S. K. Manohar, Chemical synthesis of highly conducting polypyrrole nanofiber film, *Macromolecules*, 2005, **38**, 7873–7875.

40 Z. Liu, X. Zhang, S. Poyraz, S. P. Surwade and S. K. Manohar, Oxidative template for conducting polymer nanoclips, *J. Am. Chem. Soc.*, 2010, **132**, 13158–13159.

41 K. Shu, Y. Chao, S. Chou, C. Wang, T. Zheng, S. Gambhir and G. G. Wallace, A “tandem” strategy to fabricate flexible graphene/polypyrrole nanofiber film using the surfactant-exfoliated graphene for supercapacitors, *ACS Appl. Mater. Interfaces*, 2018, **10**, 22031–22041.

42 D. P. Dubal, Z. Caban-Huertas, R. Holze and P. Gomez-Romero, Growth of polypyrrole nanostructures through reactive templates for energy storage applications, *Electrochim. Acta*, 2016, **191**, 346–354.

43 J. Zhang, X. Liu, L. Zhang, B. Cao and S. Wu, Reactive template synthesis of polypyrrole nanotubes for fabricating metal/conducting polymer nanocomposites, *Macromol. Rapid Commun.*, 2013, **34**, 528–532.

44 J. Wang, B. Wei and F. Kang, Facile synthesis of hierarchical conducting polypyrrole nanostructures via a reactive template of  $MnO_2$  and their application in supercapacitors, *RSC Adv.*, 2014, **4**, 199.

45 J. Wang, H. Liu, H. Liu, W. Hua and M. Shao, Interfacial constructing flexible  $V_2O_5$ @polypyrrole core-shell nanowire membrane with superior supercapacitive performance, *ACS Appl. Mater. Interfaces*, 2018, **10**, 18816–18823.

46 Y. Liu, L. Xiao, P. Yin and C. Zhang, One-step synthesis of polypyrrole nanofiber assemblies with enhanced electronic properties: implications for next-generation organic electronics, *ACS Appl. Nano Mater.*, 2022, **5**, 8930–8941.

47 A. Xie, F. Wu, W. Jiang, K. Zhang, M. Sun and M. Wang, Chiral induced synthesis of helical polypyrrole (PPy) nanostructures: a lightweight and high-performance material against electromagnetic pollution, *J. Mater. Chem. C*, 2017, **5**, 2175.

48 M. Sun, C. Xu, J. Li, L. Xing, T. Zhou, F. Wu, Y. Shang and A. Xie, Protonic doping brings tuneable dielectric and



electromagnetic attenuated properties for polypyrrole nanofibers, *Chem. Eng. J.*, 2020, **381**, 122615.

49 R. Elashnikov, S. Rimpelova, L. Dekanovsky, V. Svorcik and O. Lyutakov, Polypyrrole-coated cellulose nanofibers: influence of orientation, coverage and electrical stimulation on SH-SY5Y behavior, *J. Mater. Chem. B*, 2019, **7**, 6500.

50 Y. Zhou, H. Liao, Q. Qi, C. Guo, K. Qi, K. Ou, J. He, H. Wang, R. Wang and X. Chen, Polypyrrole-coated graphene oxide-doped polyacrylonitrile nanofibers for stretchable strain sensors, *ACS Appl. Nano Mater.*, 2022, **5**, 8224–8231.

51 D. P. Bhattarai, A. P. Tiwari, B. Maharjan, B. Tumurbaatar, C. H. Park and C. S. Kim, Sacrificial template-based synthetic approach of polypyrrole hollow fibers for photothermal therapy, *J. Colloid Interface Sci.*, 2019, **534**, 447–458.

52 X. Lin, Y. Bing, F. Li, H. Mei, S. Liu, T. Fei, H. Zhao and T. Zhang, An all-nanofiber-based, breathable, ultralight electronic skin for monitoring physiological signals, *Adv. Mater. Technol.*, 2022, **7**, 2101312.

53 H. Ren, T. Li, H. Wang, Z. Guo, T. Chen and F. Meng, Two birds with one stone: Superhelical chiral polypyrrole towards high-performance electromagnetic wave absorption and corrosion protection, *Chem. Eng. J.*, 2022, **427**, 131582.

54 H. He, H. Li, A. Pu, W. Li, K. Ban and L. Xu, Hybrid assembly of polymeric nanofiber network for robust and electronically conductive hydrogels, *Nat. Commun.*, 2023, **14**, 759.

55 A. P. Tiwari, T. I. Hwang, J. Oh, B. Maharjan, S. Chun, B. S. Kim, M. K. Joshi, C. H. Park and C. S. Kim, pH/NIR-responsive polypyrrole-functionalized fibrous localized drug-delivery platform for synergistic cancer therapy, *ACS Appl. Mater. Interfaces*, 2018, **10**, 20256–20270.

56 X. Sun, J. Wang, Z. Wang, C. Zhu, J. Xi, L. Fan, J. Han and R. Guo, Gold nanorod@void@polypyrrole yolk@shell nanostructures: synchronous regulation of photothermal and drug delivery performance for synergistic cancer therapy, *J. Colloid Interface Sci.*, 2022, **610**, 89–97.

57 T. Distler, C. Polley, F. Shi, D. Schneidereit, M. D. Ashton, O. Friedrich, J. F. Kolb, J. G. Hardy, R. Detsch, H. Seitz and A. R. Boccaccini, Electrically conductive and 3D-printable oxidized alginate-gelatin polypyrrole:PSS hydrogels for tissue engineering, *Adv. Healthcare Mater.*, 2021, **10**, 2001876.

58 Y. Liang, A. Mitiashkin, T. T. Lim and J. C. Goh, Conductive polypyrrole encapsulated silk fibroin fibers for cardiac tissue engineering, *Biomaterials*, 2021, **276**, 121008.

59 B. Maharjan, V. K. Kaliannagounder, S. R. Jang, G. P. Awasthi, D. P. Bhattarai, G. Choukrani, C. H. Park and C. S. Kim, In-situ polymerized polypyrrole nanoparticles immobilized poly( $\epsilon$ -caprolactone) electrospun conductive scaffolds for bone tissue engineering, *Mater. Sci. Eng. C*, 2020, **114**, 111056.

60 S. D. Dutta, K. Ganguly, A. Randhawa, T. V. Patil, D. K. Patel and K. Lim, Electrically stimulated 3D bioprinting of gelatin-polypyrrole hydrogel with dynamic semi-IPN network induces osteogenesis via collective signaling and immunopolarization, *Biomaterials*, 2023, **294**, 121999.

61 R. Bashyam and P. Zelenay, A class of non-precious metal composite catalysts for fuel cells, *Nature*, 2006, **443**, 63–66.

62 F. M. Guo, R. Q. Xu, X. Cui, L. Zhang, K. L. Wang, Y. W. Yao and J. Q. Wei, High performance of stretchable carbon nanotube-polypyrrole fiber supercapacitors under dynamic deformation and temperature variation, *J. Mater. Chem. A*, 2016, **4**, 9311–9318.

63 J. Wang, Z. Wen, Y. Zi, L. Lin, C. Wu, H. Guo, Y. Xi, Y. Xu and Z. L. Wang, Self-powered electrochemical synthesis of polypyrrole from the pulsed output of a triboelectric nanogenerator as a sustainable energy system, *Adv. Funct. Mater.*, 2016, **26**, 3542–3548.

64 P. C. Lohani, A. P. Tiwari, K. Chhetri, A. Muthurasu, B. Dahal, S. Chae, T. H. Ko, J. Y. Lee, Y. S. Chung and H. Y. Kim, Polypyrrole nanotunnels with luminal and abluminal layered double hydroxide nanosheets grown on a carbon cloth for energy storage applications, *ACS Appl. Mater. Interfaces*, 2022, **14**, 23285–23296.

65 Y. Wang, K. Bian, C. Hu, Z. Zhang, N. Chen, H. Zhang and L. Qu, Flexible and wearable graphene/polypyrrole fibers towards multifunctional actuator applications, *Electrochem. Commun.*, 2013, **35**, 49–52.

66 J. D. Madden, R. A. Cush, T. S. Kanigan and I. W. Hunter, Fast contracting polypyrrole actuators, *Synth. Met.*, 2000, **113**, 185–192.

67 M. Zou, S. Li, X. Hu, X. Leng, R. Wang, X. Zhou and Z. Liu, Progresses in tensile, torsional, and multifunctional soft actuators, *Adv. Funct. Mater.*, 2021, **31**, 2007437.

68 M. Brinker, G. Dittrich, C. Richert, P. Lakner, T. Krekeler, T. F. Keller, N. Huber and P. Huber, Giant electrochemical actuation in a nanoporous silicon-polypyrrole hybrid material, *Sci. Adv.*, 2020, **6**, eaba1483.

69 R. Jain, N. Jadon and A. Pawaiya, Polypyrrole based next generation electrochemical sensors and biosensors: a review, *Trends Anal. Chem.*, 2017, **97**, 363–373.

70 A. Ho-Pun-Cheung, S. Choblet, T. Colineau, H. Abaibou, D. Zsoldos, K. Brengel-Pesce, J. Grenier, P. Cleuziat and E. Lopez-Crapez, Detection of single nucleotide polymorphisms by minisequencing on a polypyrrole DNA chip designed for medical diagnosis, *Lab. Invest.*, 2006, **86**, 304–313.

71 R. Khoder and H. Korri-Youssoufi, E-DNA biosensors of *M. tuberculosis* based on nanostructured polypyrrole, *Mater. Sci. Eng. C*, 2020, **108**, 110371.

72 H. Jia, J. Wang, X. Zhang and Y. Wang, Pen-writing polypyrrole arrays on paper for versatile cheap sensors, *ACS Macro Lett.*, 2014, **3**, 86–90.

73 M. R. Miah, M. Yang, S. Khandaker, M. M. Bashar, A. K. D. Alsukaibi, H. M. A. Hassan, H. Znad and M. R. Awual, Polypyrrole-based sensors for volatile organic compounds (VOCs) sensing and capturing: A comprehensive review, *Sens. Actuators, A*, 2022, **347**, 113933.

